Algorithmica (2019) 81:2046–2071
https://doi.org/10.1007/s00453-018-0523-5

On Smooth Orthogonal and Octilinear Drawings: Relations, Complexity and Kandinsky Drawings

Michael A. Bekos[1] · Henry Förster[1] · Michael Kaufmann[1]

Received: 12 September 2017 / Accepted: 9 October 2018 / Published online: 22 October 2018

Abstract
We study two variants of the well-known orthogonal graph drawing model: (1) the smooth orthogonal, and (2) the octilinear. Both models are extensions of the orthogonal one, by supporting one additional type of edge segments (circular arcs and diagonal segments, respectively). For planar graphs of maximum vertex degree 4, we analyze relationships between the graph classes that can be drawn bendless in the two models and we also prove $\mathcal{NP}$-hardness for a restricted version of the bendless drawing problem for both models. For planar graphs of higher vertex degree, we present an algorithm that produces bi-monotone smooth orthogonal drawings with at most two segments per edge, which also guarantees a linear number of edges with exactly one segment.

Keywords Graph drawing · Smooth orthogonal · Octilinear

1 Introduction

Orthogonal graph drawing is an intensively studied and well established model for drawing graphs [15,31]. As a result, several efficient algorithms providing good aesthetics and good readability have been proposed over the years, see e.g., [8,23,33,39]. In such drawings, each vertex corresponds to a point on the Euclidean plane and each

A preliminary version of this article has appeared in the proceedings of the 25th International Symposium on Graph Drawing and Network Visualization [2].

✉ Henry Förster
foersth@informatik.uni-tuebingen.de

Michael A. Bekos
bekos@informatik.uni-tuebingen.de

Michael Kaufmann
mk@informatik.uni-tuebingen.de

1 Wilhelm-Schickard-Institut für Informatik, Universität Tübingen, Tübingen, Germany

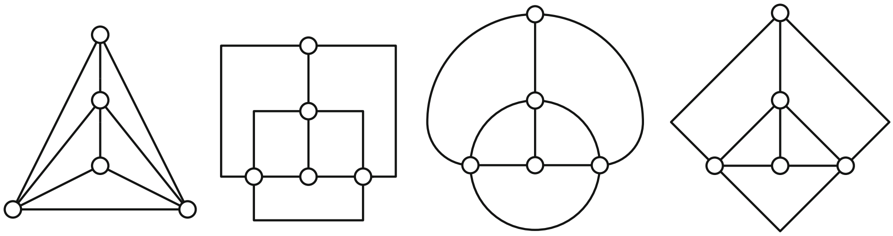

Fig. 1 Different drawings of a planar graph of maximum vertex degree 4: **a** straight-line, **b** orthogonal 3-drawing, **c** smooth orthogonal 2-drawing, and **d** octilinear 2-drawing

edge is drawn as an alternating sequence of axis-aligned line segments; refer to Fig. 1b for an example.

Several research directions build upon this successful model. In this work, we focus on two models that have recently received attention. The first one is the *smooth orthogonal* [5], in which every edge is a sequence of axis-aligned segments and circular arc segments with common axis-aligned tangents (i.e., quarter, half or three-quarter circular arc segments); refer to Fig. 1c for an example. The second model is the *octilinear* [3], in which every edge is a sequence of axis-aligned and diagonal (at $\pm 45°$) segments; refer to Fig. 1d for an example. In the orthogonal and in the smooth orthogonal models, each edge may enter a vertex using one out of four available (axis-aligned) directions, called *ports*. Thus both models support graphs of maximum vertex degree 4. In the octilinear model, each vertex has eight available ports that are equispaced around each vertex and therefore one can draw graphs of maximum vertex degree 8.

Observe that both models extend the orthogonal by allowing one more type of edge-segments (circular arcs and diagonal segments, respectively). The smooth orthogonal drawing model was introduced with the aim of combining the artistic appeal of *Lombardi drawings* [18,21] with the clarity and rigidity of the orthogonal drawings. The octilinear drawing model, on the other hand, is primarily motivated by metro-map and map schematization applications (see, e.g., [28,35,36,38]).

For readability purposes, usually in such drawings one seeks to minimize the *edge complexity* [15,31], that is, the maximum number of segments used for representing any edge in the drawing. Also, when the input is a planar graph, one naturally seeks for a corresponding planar drawing. Note that drawings with edge complexity 1 are also called *bendless*. For simplicity, we refer to drawings with edge complexity k as k*-drawings*; thus, by definition, orthogonal and octilinear k-drawings have at most $k-1$ bends per edge.

Known Results There exists a plethora of results for each of the aforementioned models; here we overview existing results for drawings with low edge complexity. For a more detailed overview, we point the reader to [40].

– All planar graphs of maximum vertex degree 4, except for the octahedron, admit orthogonal 3-drawings; the octahedron is orthogonal 4-drawable [8,33]. All planar graphs of maximum vertex degree 3 admit orthogonal 2-drawings [30]. Minimizing the number of bends over all embeddings of a planar graph of maximum vertex degree 4 is $\mathcal{NP}$-hard [26]. For a given planar embedding, however, finding a planar orthogonal drawing with minimum number of bends can be done in polynomial time by an approach, called *topology-shape-metrics* [39]. The core of this approach is based on min-cost flow computations and works in three phases. Initially, a planar embedding is computed unless specified by the input (*topology phase*). In the next phase, called *shape phase*, the angles and the bends of the drawing are computed, yielding an *orthogonal representation*. In the last phase, called *metrics phase*, the actual coordinates for the vertices and bends are computed. For more details, we point the reader to [19].

- All planar graphs of maximum vertex degree 4 (including the octahedron) admit smooth orthogonal 2-drawings. Note that not all planar graphs of maximum vertex degree 4 allow for bendless smooth orthogonal drawings [5], and that such drawings may require exponential area [1]. Bendless smooth orthogonal drawings are possible only for subclasses, e.g., for planar graphs of maximum vertex degree 3 [4] and for outerplanar graphs of maximum vertex degree 4 [1]. It is worth mentioning that the complexity of the recognition problem, whether a planar graph of maximum vertex degree 4 admits a bendless smooth orthogonal drawing, has not been settled (it is conjectured to be $\mathcal{NP}$-hard [1]).
- All planar graphs of maximum vertex degree 8 admit octilinear 3-drawings [32], while planar graphs of maximum vertex degree 4 and 5 allow for octilinear 2-drawings in cubic and super-polynomial area, respectively [3]. Bendless octilinear drawings are always possible for planar graphs of maximum vertex degree 3 [17, 29]. Note that deciding whether an embedded planar graph of maximum vertex degree 8 admits a bendless octilinear drawing is $\mathcal{NP}$-hard [35]. It is not, however, known whether this negative result applies for planar graphs of maximum vertex degree 4 or whether these graphs allow for a decision algorithm; in fact, there exist planar graphs of maximum vertex degree 4 that do not admit bendless octilinear drawings [6].

Our Contribution We study smooth orthogonal and octilinear drawings of planar graphs with small edge complexity. Our results are summarized as follows:

- Motivated by the fact that usually one can "easily" convert a smooth orthogonal drawing of a planar graph of maximum vertex degree 4 to a corresponding octilinear one (e.g., by replacing quarter circular arc segments with diagonal edge segments; see Fig. 1c–d for an example), and vice versa, we study in Sect. 3 inclusion-relationships between the graph-classes that admit such drawings. Our findings are also summarized in Fig. 3.
- In Sect. 4, we show that it is $\mathcal{NP}$-hard to decide whether an embedded planar graph of maximum vertex degree 4 admits a bendless smooth orthogonal or a bendless octilinear drawing, in the case where the angles between any two edges incident to a common vertex and the shapes of all edges are specified as part of the input (e.g., as in the last step of the topology-shape-metrics approach [39]). Our proof is a step towards settling the complexities of both decision problems in their general form. Note that, our $\mathcal{NP}$-hardness result shows that the last step of the topology-shape-metrics approach is hard, if considered in isolation in the smooth

orthogonal model or in the octilinear model, while in the classic orthogonal model it can be solved efficiently using network flows. This observation suggests that the topology-shape-metrics approach is suitable for neither of the two models.

- Inspired by the *Kandinsky model* (see, e.g., [7,14,23]) for drawing planar graphs of arbitrary vertex degree in an orthogonal style, we present in Sect. 5 two drawing algorithms that yield smooth orthogonal drawings of good quality, that are also bi-monotone, i.e., each edge is drawn xy-monotone. More precisely, the first yields drawings of quadratic area, which can also be transformed into octilinear with bends at 135°, while maintaining the area consumption asymptotically unchanged. The second algorithm yields drawings of cubic area but at the same time guarantees that at most $2n - 5$ edges are drawn with two segments.

Before we proceed with the detailed description of our algorithms, we introduce in Sect. 2 preliminary notions and definitions; for a list of open problems raised by our work refer to Sect. 7.

2 Preliminary Notions and Definitions

Unless otherwise specified, we consider simple undirected graphs. Let $G = (V, E)$ be such a graph. We denote by n and m the number of vertices and edges of G, respectively. We denote by $d(v)$ the vertex degree of a vertex $v \in V$, that is, the number of its incident edges. We say that G has *maximum vertex degree* Δ, if G has no vertex with degree larger than Δ, that is, $d(v) \leq \Delta$ for each $v \in V$.

A *drawing* Γ of G is a function that maps each vertex $v \in V$ to a distinct point p_v in $\mathbb{R}^2$, and each edge $(u, v) \in E$ to a simple open Jordan curve connecting p_u and p_v. Drawing Γ is *planar* if no two edges cross. A graph is *planar* if it admits a planar drawing. A planar drawing Γ of G partitions the plane into topologically connected regions, called *faces*; the unbounded face is called *outerface*. A (*topological*) *planar embedding* $\mathcal{E}$ of G is an equivalence class of planar drawings that define the same set of faces. Embedding $\mathcal{E}$ can also be defined by the cyclic orders of the edges incident to each vertex (also called *combinatorial embedding*). For a deeper introduction to graph theoretic basics and to planar graphs, we point the reader to [15,27].

We assume familiarity with standard graph drawing techniques, such as the *canonical ordering* [13,30] and the *shift-method* by de Fraysseix, Pach and Pollack [13], which we also outline in the following.

The *canonical ordering* for maximal planar graphs [13] is defined as follows. Let $G = (V, E)$ be a maximal planar graph and let $\pi = (v_1, \ldots, v_n)$ be a permutation of V. Assume that edges (v_1, v_2), (v_2, v_n) and (v_1, v_n) form a face of G, which we assume w.l.o.g. to be its outerface. For $k = 1, \ldots, n$, let G_k be the subgraph induced by $\cup_{i=1}^{k}\{v_i\}$ and denote by C_k the outerface of G_k. Then, π is a *canonical ordering* of G if for each $k = 2, \ldots, n$ the following hold:

(i) G_k is biconnected,
(ii) all neighbors of v_k in G_{k-1} are (consecutive) on C_{k-1}, and
(iii) if $k \neq n$, then v_k has at least one neighbor v_j, with $j > k$.

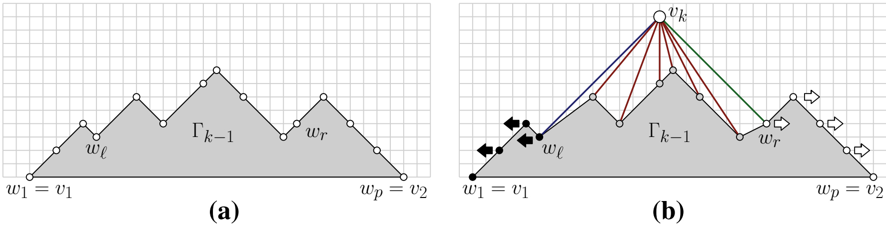

Fig. 2 Illustration of the shift-method by de Fraysseix, Pach and Pollack [13]. **a** Contour condition. **b** Placement of v_k in Γ_{k-1}

It is known that a canonical ordering of a maximal planar graph can be computed in linear time [30].

The *shift-method* [13] is a well-known incremental algorithm, which constructs in linear time a planar drawing Γ of a maximal planar graph $G = (V, E)$. Drawing Γ has integer grid coordinates and requires quadratic area. More precisely, based on a canonical order π of G, drawing Γ is constructed as follows. Initially, vertices v_1, v_2 and v_3 are placed at points (0, 0), (2, 0) and (1, 1). For $k = 4, \dots, n$, assume that a planar drawing Γ_{k-1} of G_{k-1} has been constructed in which each edge of C_{k-1} is drawn as a straight-line segment with slope ± 1, except for the edge (v_1, v_2), which is drawn as a horizontal line segment (*contour condition*; see Fig. 2a). Also, assume that each of the vertices $v_1, \dots, v_{k-1}$ has been associated with a so-called *shift-set*, which for v_1, v_2 and v_3 are singletons containing only themselves. Let $(w_1, \dots, w_p)$ be the vertices of C_{k-1} from left to right in Γ_{k-1}, where $w_1 = v_1$ and $w_p = v_2$. For $i = 1, \dots, p$, denote by $S(w_i)$ the shift-set of w_i. Let $(w_\ell, \dots, w_r)$, with $1 \leq \ell < r \leq p$ be the neighbors of v_k from left to right along C_{k-1} in Γ_{k-1}. To avoid edge-overlaps, the algorithm first translates each vertex in $\cup_{i=1}^{\ell} S(w_i)$ one unit to the left and each vertex in $\cup_{i=r}^{p} S(w_i)$ one unit to the right. Then, the algorithm places vertex v_k at the intersection of the line with slope $+1$ through w_ℓ with the line with slope -1 through w_r and sets the shift-set of v_k to $\{v_k\} \cup_{i=\ell+1}^{r-1} S(w_i)$; see Fig. 2b.

3 Relationships Between Graph Classes

In this section, we consider relationships between the classes of graphs that admit smooth orthogonal k-drawings and octilinear k-drawings, where $k \geq 1$. For the sake of simplicity, we denote these two classes by SC_k and $8C_k$, respectively. Our findings are also summarized in Fig. 3.

By definition, $SC_1 \subseteq SC_2$ and $8C_1 \subseteq 8C_2 \subseteq 8C_3$ hold. Since each planar graph of maximum vertex degree 8 admits an octilinear 3-drawing [32], class $8C_3$ coincides with the class of planar graphs of maximum vertex degree 8. Similarly, class SC_2 coincides with the class of planar graphs of maximum vertex degree 4, because these graphs admit smooth orthogonal 2-drawings [1]. This also implies that $SC_2 \subseteq 8C_2$, since each planar graph of maximum vertex degree 4 admits an octilinear 2-drawing [3]. The relationship $8C_2 \neq 8C_3$ follows from [3], where it was proven that there exist planar graphs of maximum vertex degree 6 that do not admit octilinear 2-drawings. The

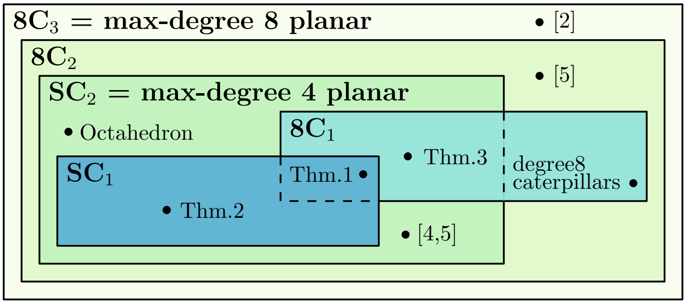

Fig. 3 Different inclusion-relationships: for $k \geq 1$, SC_k and $8C_k$ correspond to the classes of graphs that admit smooth orthogonal and octilinear k-drawings, respectively

relationship $SC_2 \neq 8C_2$ follows from [6], where it was shown that there exist planar graphs of maximum vertex degree 5 that admit octilinear 2-drawings and no octilinear 1-drawings, and the fact that planar graphs of maximum vertex degree 5 cannot be drawn in the smooth orthogonal model. The octahedron graph admits neither a bendless smooth orthogonal drawing [5] nor a bendless octilinear drawing [6]. However, since it is of maximum vertex degree 4, it admits 2-drawings in both models [1,3]. Hence, it belongs to $8C_2 \cap SC_2 \setminus (8C_1 \cup SC_1)$. To prove that $8C_1 \setminus SC_2 \neq \emptyset$, observe that a caterpillar whose spine vertices are of degree 8 clearly admits an octilinear 1-drawing, however, due to its vertex degree it does not admit a smooth orthogonal drawing.

To complete the discussion of the relationships of Fig. 3, we have to show that SC_1 and $8C_1$ are incomparable. This is the most interesting part of our proof, since as already mentioned, usually one can "easily" convert a smooth orthogonal drawing of a planar graph of maximum vertex degree 4 to a corresponding octilinear one (e.g., by replacing quarter circular arc segments with diagonal edge segments; see Fig. 1c–d for an example), and vice versa. Since the endpoints of each edge of a bendless smooth orthogonal or octilinear drawing are along a line with slope 0, 1, -1 or ∞, such conversions are in principle possible. Two difficulties that might arise are to preserve planarity and to guarantee that no two edges enter a vertex using the same port. However, there exist infinitely many (even 4-regular) planar graphs that admit drawings in both models, as we formally prove in the following theorem.

Theorem 1 *There is an infinitely large family of* 4*-regular planar graphs that admit both bendless smooth orthogonal and bendless octilinear drawings.*

Proof For each $k \in \mathbb{N}_+$ we describe a 4-regular planar graph $G_k = (V_k, E_k)$ with $20k$ vertices that admits both a bendless smooth orthogonal drawing and a bendless octilinear drawing; refer to Fig. 4 for the case $k = 2$. Graph G_k has $4k$ subgraphs $W_{i,j}$ such that $1 \leq i \leq 2k$ and $j \in \{t, b\}$, where t and b stand for *top* and *bottom*, respectively. Graph $W_{i,j}$ consists of five vertices $c_{i,j}$, $n_{i,j}$, $w_{i,j}$, $e_{i,j}$, and $s_{i,j}$, such that $W_{i,j}$ is a wheel on five vertices, where $c_{i,j}$ is its center-vertex and cycle $C_{i,j} = (n_{i,j}, w_{i,j}, s_{i,j}, e_{i,j})$ is its rim. Vertices $n_{i,j}$, $w_{i,j}$, $s_{i,j}$ and $e_{i,j}$ are the *north*, *west*, *south* and *east* vertices of $C_{i,j}$, respectively.

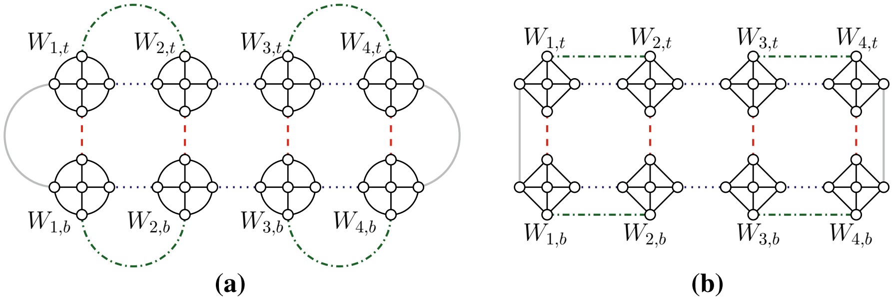

Fig. 4 Illustrations for the proof of Theorem 1 depicting drawings of G_2. **a** A smooth orthogonal 1-drawing. **b** An octilinear 1-drawing

All vertices $c_{i,j}$ already have degree four, but every other vertex has degree three. So, in the following, we only describe the edges that will make graph G_k 4-regular. For $1 \leq h \leq 2k-1$ and $j \in \{t, b\}$, $(e_{h,j}, w_{h+1,j}) \in E_k$; dotted edges in Fig. 4. Also, $(w_{1,t}, w_{1,b}) \in E_k$ and $(e_{2k,t}, e_{2k,b}) \in E_k$; gray edges in Fig. 4. For $1 \leq h \leq 2k$, $(s_{h,t}, n_{h,b}) \in E_k$; dashed edges in Fig. 4. Finally, for $1 \leq h \leq k$, $(n_{2h-1,t}, n_{2h,t}) \in E_k$ and $(s_{2h-1,b}, s_{2h,b}) \in E_k$; dashed dotted edges in Fig. 4. With those additional edges, G_k becomes 4-regular. Figure 4 is a certificate that $G_k = (V_k, E_k)$ indeed admits both a bendless smooth orthogonal drawing and a bendless octilinear drawing. □

To complete the discussion of the inclusion relationships of Fig. 3, we show in the next two theorems that SC_1 and $8C_1$ are incomparable.

Theorem 2 *There are infinitely many* 4*-regular planar graphs that admit bendless smooth orthogonal drawings but no bendless octilinear drawing.*

Proof Consider the planar graph C of Fig. 5a, which is drawn bendless smooth orthogonal. We claim that C admits no bendless octilinear drawing. If one substitutes its degree-2 vertex (denoted by c in Fig. 5a) by an edge connecting its two neighbors, then the resulting graph is triconnected, which implies that it admits a unique embedding (up to the choice of its outerface; see Fig. 5a–b). Now, observe that the outerface of any octilinear drawing of graph C (if any) has length at most 5 (Constraint 1). In addition, each vertex of this outerface (except for c, which is of degree 2) must have two ports pointing in the interior of this drawing, because every vertex of C is of degree 4, except for c. This implies that the angle formed by any two consecutive edges of this outerface is at most 225°, except for the pair of edges incident to c (Constraint 2). But if we want to satisfy both constraints, then at least one edge of this outerface must be drawn with a bend; see Fig. 5c. Hence, graph C does not admit a bendless octilinear drawing.

Based on graph C, for each $k \in \mathbb{N}_0$ we construct a 4-regular planar graph G_k consisting of $k+2$ biconnected components $C_1, \ldots, C_{k+2}$ arranged in a *chain*; see Fig. 5d for the case $k = 1$. Clearly, graph G_k admits a bendless smooth orthogonal drawing for any k. Since components C_1 and C_{k+2} are isomorphic to graph C, graph G_k does not admit a bendless octilinear drawing for any k. □

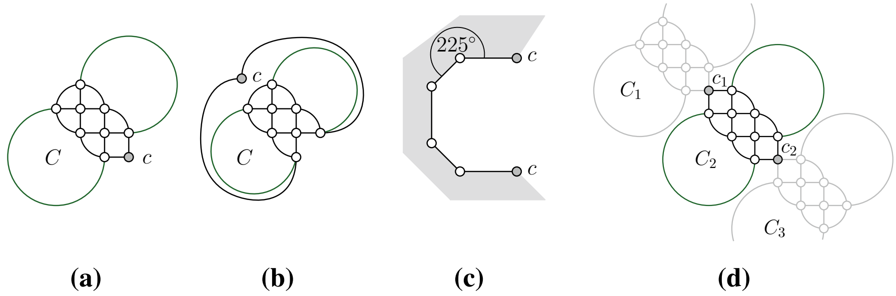

Fig. 5 Illustrations for the proof of Theorem 2

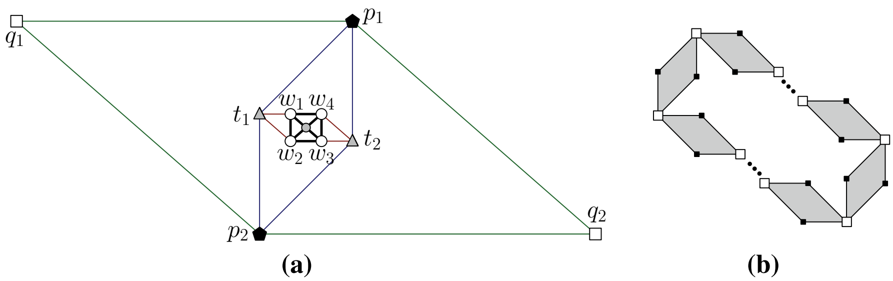

Fig. 6 Illustrations for the proof of Theorem 3

Theorem 3 *There are infinitely many 4-regular planar graphs that admit bendless octilinear drawings but no bendless smooth orthogonal drawing.*

Proof Consider the planar graph B of Fig. 6a, which is drawn bendless in the octilinear model. First, we discuss some structural properties of graph B. Observe that graph B contains a wheel on five vertices as a subgraph, call it W_5, which is induced by the vertices drawn as circles in Fig. 6a. Its center is vertex c (gray colored in Fig. 6a) and its rim consists of vertices w_1, w_2, w_3, and w_4. Vertices w_1 and w_2 form a triangular face with vertex t_1; analogously, vertices w_3 and w_4 form a triangular face with t_2 (vertices t_1 and t_2 are drawn as triangles in Fig. 6a). Observe that t_1 and t_2 form a separation pair and both are connected to vertices p_1 and p_2 (drawn as pentagons in Fig. 6a) forming two pentagonal faces $(p_1, t_1, w_1, w_4, t_2)$ and $(p_2, t_2, w_3, w_2, t_1)$. Observe that p_1 and p_2 also form a separation pair and are both connected to vertices q_1 and q_2 (drawn as squares in Fig. 6a) forming two quadrilateral faces (q_1, p_2, t_1, p_1) and (q_2, p_1, t_2, p_2). Hence, B has two separation pairs and two vertices of degree 2 (that is, q_1 and q_2). The remaining vertices of B have degree exactly 4.

For each $k \in \mathbb{N}_0$ we construct a 4-regular planar graph G_k consisting of $2k + 4$ copies of B arranged in a cycle; refer to Fig. 6b where each copy of B is drawn as a gray-shaded parallelogram. By construction, graph G_k admits a bendless octilinear drawing, for any k. By planarity, at least one copy of graph B must be embedded with the outerface (p_1, q_1, p_2, q_2) such that each of q_1 and q_2 has two unoccupied ports incident to this outerface. However, under this restriction the embedding of this particular copy of B must be isomorphic to the one of Fig. 6a. We now proof that, for

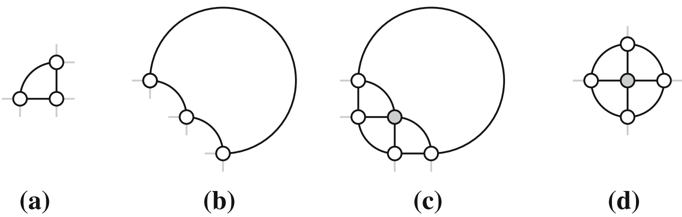

Fig. 7 All smooth orthogonal drawings **a**–**b** of a triangular face, and **c**, **d** of a wheel on five vertices, such that all unoccupied ports are on the outerface of the drawing

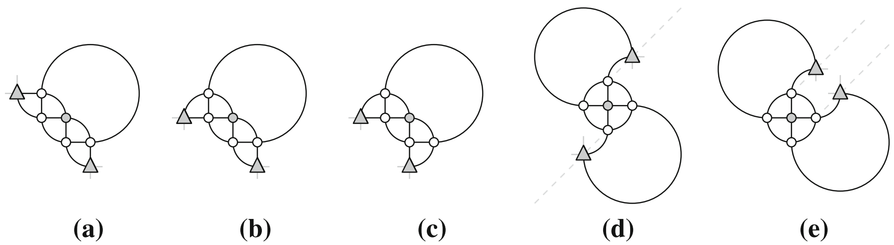

Fig. 8 All smooth orthogonal drawings of the subgraph of graph B induced by wheel W_5, and vertices t_1 and t_2, such that all unoccupied ports are on the outerface of the drawing

any k, graph G_k does not admit a bendless smooth orthogonal drawing by showing that graph B does not admit a bendless smooth orthogonal drawing, when its outerface is (p_1, q_1, p_2, q_2) and each of q_1 and q_2 has two unoccupied ports incident to this outerface.

First, we observe the following: If we want to draw wheel W_5, such that all of its unoccupied ports are on its outerface, then none of its four triangular faces must have an unoccupied port pointing in its interior. In the bendless smooth orthogonal model, there are only two possible drawings for a triangular face fulfilling this property (as shown in [1]), which are illustrated in Fig. 7a, b. This implies that W_5 admits only two bendless smooth orthogonal drawings such that all of its unoccupied ports are on its outerface, which are illustrated in Fig. 7c, d.

Next, we consider vertices t_1 and t_2. Since each of them defines a triangular face in the subgraph induced by wheel W_5, and vertices t_1 and t_2, we can conclude similar as above, that there are five different drawings of this graph, which are illustrated in Fig. 8. Note that in Fig. 8d, e both t_1 and t_2 can independently move along the gray colored diagonal rays.

In the following, we consider all candidate positions for p_1 and p_2, which we can identify adopting the following simple rule. In a bendless smooth orthogonal drawing, both endpoints of an edge are located along a horizontal, vertical or diagonal line. Both p_1 and p_2 are neighbors of both t_1 and t_2, for which we already defined their locations. If we consider all rays emanating from t_1 and t_2 with slopes $\{0, 1, -1, \infty\}$, then p_1 and p_2 must be located at an intersection of a ray emanating from t_1 and a ray emanating from t_2. Following this rule, we enumerate in Figs. 9 and 10 all possible candidate positions for p_1 and p_2; refer to the gray-colored pentagons. Note that the case illustrated in Fig. 8e has several subcases to be considered depending on the

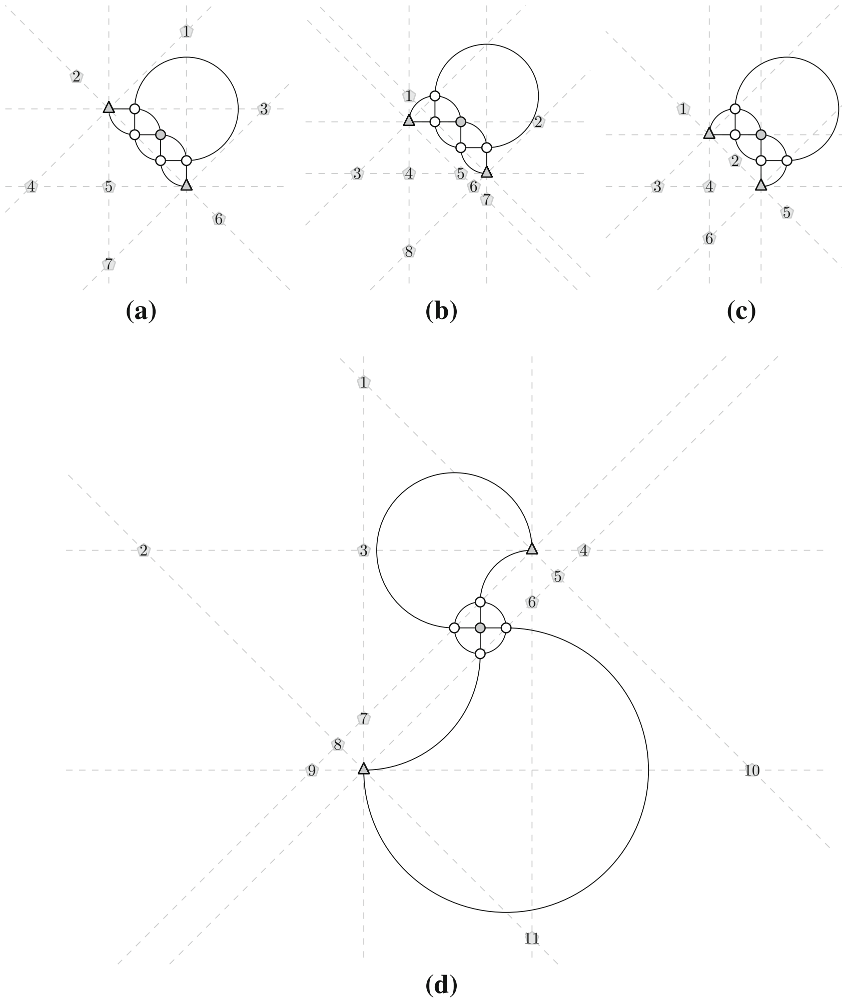

Fig. 9 An enumeration of the candidate positions for p_1 and p_2 that occur for the cases of: **a** Fig. 8a, **b** Fig. 8b, **c** Fig. 8c, and **d** Fig. 8d

relative positioning of t_1 and t_2. We illustrate them in Fig. 10a, where we have assumed that the position of one of t_1 and t_2 is fixed, and then we enumerate how the second one is positioned with respect to the first. Observe that some cases are symmetric with respect to the diagonal line through the center of the wheel (in Fig. 10a, symmetric cases have the same number). In Fig. 10b–e, we illustrate the non-symmetric ones (that are marked with an asterisk in Fig. 10a). More precisely, Fig. 10b illustrates the case where t_1 and t_2 are diagonally aligned; Fig. 10c illustrates the case where t_1 and t_2 are vertically aligned (which is symmetric to the case where they are horizontally aligned); Figs 10d, e illustrate the remaining two cases of Fig. 10a.

For each candidate position, we then try to draw the edges from t_1 and t_2 to p_1 and p_2 using one of the edge segments supported by the smooth orthogonal model.

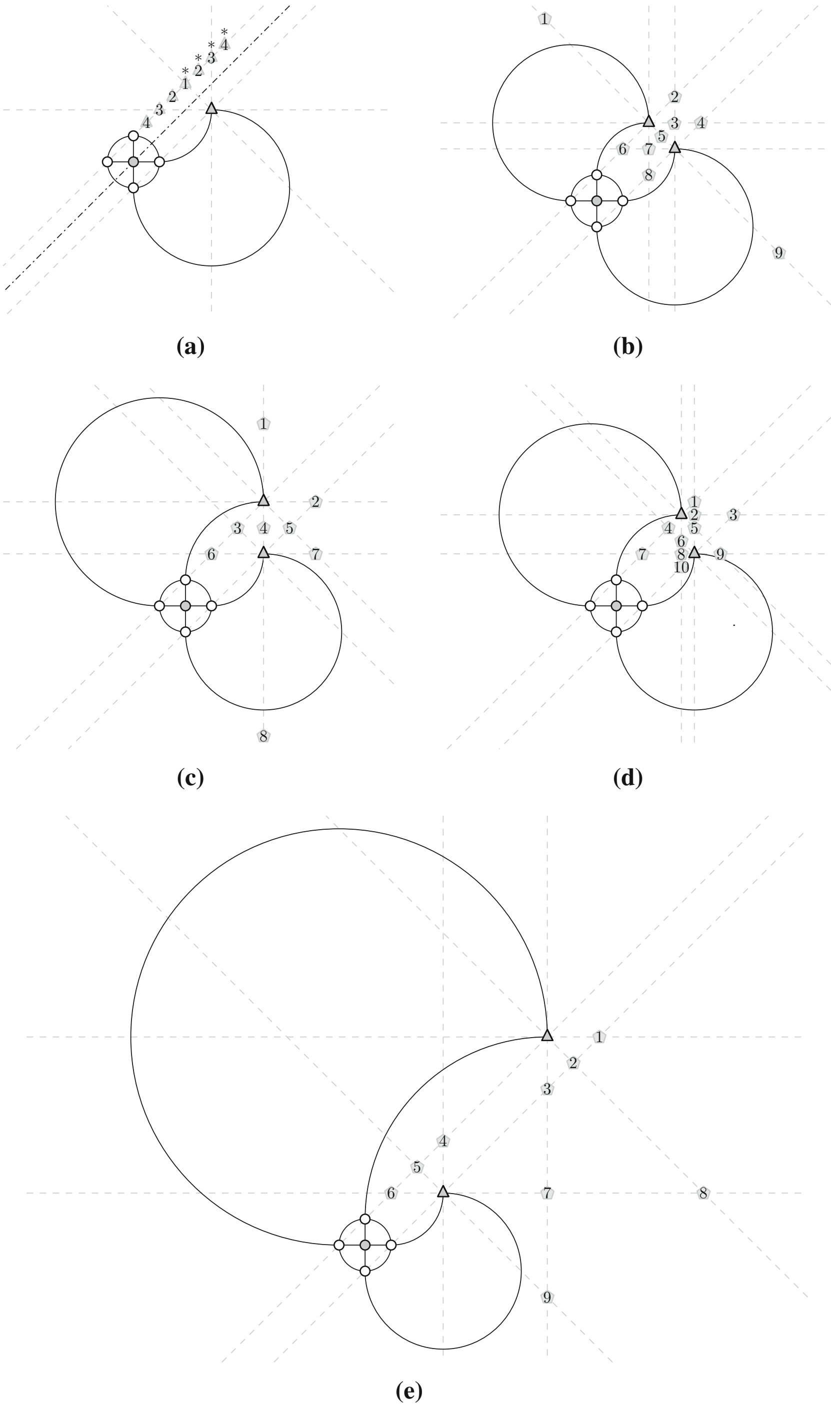

Fig. 10 An enumeration of the candidate positions for p_1 and p_2 that occur for the cases of Fig. 8e

Table 1 An overview of the forbidden patterns (FP) occurring when placing p_1 and p_2 at each of the candidate positions as they are enumerated in Figs. 9 and 10; the gray-colored cell of this table illustrates the forbidden patterns occurring when placing q_1 and q_2 at each of the candidate positions of Fig. 11, which illustrates the only valid drawing derived by placing p_1 and p_2 at positions 2 and 6 of Fig. 9a

Case	Position / Forbidden Pattern											
Figure 9a	Position:	1	2	3	4	5	6	7				
	FP.:	III	–	III	III	III	–	III				
Figure 9b	Position:	1	2	3	4	5	6	7	8			
	FP.:	III	II	–	III	III	III	–	–			
Figure 9c	Position:	1	2	3	4	5	6					
	FP.:	III	III	III	–	III	III					
Figure 9d	Position:	1	2	3	4	5	6	7	8	9	10	11
	FP.:	III	II	II	III	III	I	I	III	III	II	III
Figure 10b	Position:	1	2	3	4	5	6	7	8	9		
	FP.:	I	II	III	II	–	II	III	II	I		
Figure 10c	Position:	1	2	3	4	5	6	7	8			
	FP.:	I	II	III	–	III	II	II	I			
Figure 10d	Position:	1	2	3	4	5	6	7	8	9	10	
	FP.:	II	III	II	III	III	III	II	III	II	II	
Figure 10e	Position:	1	2	3	4	5	6	7	8	9		
	FP.:	II	III	III	III	III	II	III	II	II		
Figure 11	Position:	1	2	3	4	5	6	7	8	9		
	FP.:	I	III	III	I	I	III	I	III	I		

The resulting drawing is *valid* if and only if none of the following *forbidden patterns* appears:

FP.I. an edge is involved in crossings (as planarity is deviated),
FP.II. a port of a vertex is used twice (as this is not permitted by our model),
FP.III. a vertex has an unoccupied port not incident to the outerface (as this will not allow adding q_1 or q_2).

Otherwise, the resulting drawing is *invalid*. Note that in Figs. 9d and 10 we have appropriately chosen the radii of the arcs incident to t_1 and t_2, so to avoid a position for p_1 and p_2 to become invalid due to Forbidden Pattern I.

For each candidate position as it is enumerated in each subfigure of Figs. 9 and 10, we demonstrate in Table 1 whether it leads to some forbidden pattern. It is immediate to see from Table 1 that all candidate positions for placing p_1 and p_2 that are obtained from the cases illustrated in Figs. 9c–d and b–e yield Forbidden Pattern I, II or III, except for Position 4 of Fig. 9c, Position 5 of Fig. 10b and Position 4 of Fig. 10c. These particular positions do not yield any forbidden pattern. However, since we have to place two vertices (namely, p_1 and p_2), only one of them can be placed without introducing a forbidden pattern; the other will inevitably introduce one.

It remains to discuss the candidate positions for placing p_1 and p_2 that are obtained from the cases illustrated in Fig. 9a, b. As demonstrated in Table 1, the former has two candidate positions (namely, Positions 2 and 6), which do not yield any forbidden

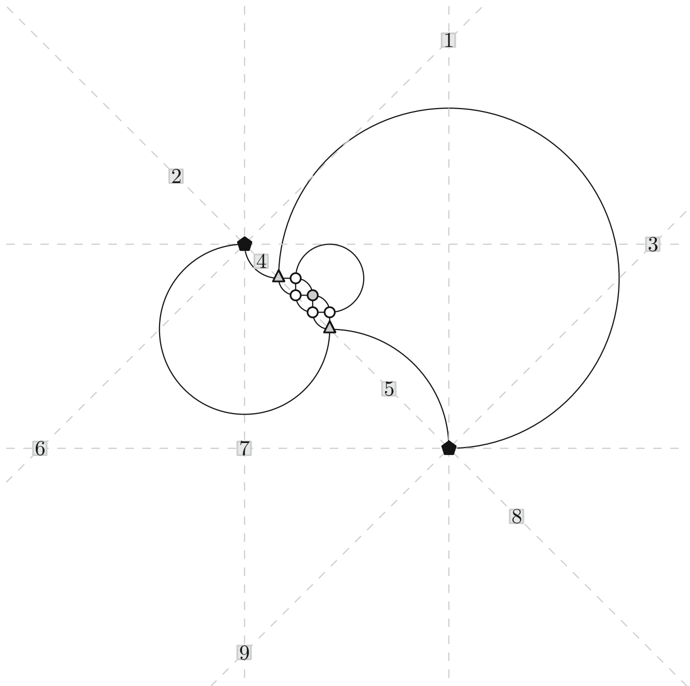

Fig. 11 An enumeration of the candidate positions for placing q_1 and q_2, when p_1 and p_2 have been placed at positions 2 and 6 of Fig. 9a, respectively

pattern; the latter case has three such candidate positions (namely, Positions 3, 7 and 8). We consider the latter case first. By combining the three candidate positions for both p_1 and p_2, we can conclude that there exist in total three different placement combinations for p_1 and p_2. However, it is not difficult to see that all three of them yield Forbidden Pattern II. Regarding the former case, we observe that by placing p_1 and p_2 at Positions 2 and 6 of Fig. 9a, respectively (which are the only ones not introducing any forbidden pattern), we obtain a valid drawing. This drawing is illustrated in Fig. 11.

We proceed by considering all possible candidate positions for placing q_1 and q_2, as we did for p_1 and p_2; refer to the gray-colored squares in Fig. 11 for an enumeration of all cases. Note that in Fig. 11 we have appropriately chosen the radii of the arcs incident to p_1 and p_2, so to avoid a position for q_1 and q_2 to become invalid due to Forbidden Pattern I. In the last (shaded in gray) row of Table 1, we demonstrate that each candidate position for placing q_1 and q_2 yields either Forbidden Pattern I or III. As a result, we can conclude that neither q_1 nor q_2 can be added to the only valid drawing for p_1 and p_2 of Fig. 11, which completes the proof of this theorem. □

4 $\mathcal{NP}$-Hardness Results

In this section, we study the complexity of the bendless smooth orthogonal and octilinear drawing problems. As a first step towards addressing the complexity of both problems for planar graphs of maximum vertex degree 4 in general, here we make an additional assumption. We assume that the input, apart from an embedding, also specifies a *smooth orthogonal* or an *octilinear representation*, which are defined analogously to the orthogonal ones: (i) the angles between consecutive edges incident to a common vertex in the cyclic order around it (given by the planar embedding) are specified, and (ii) the *shape* of each edge (e.g., straight-line, or quarter circular arc) is also specified. In other words, we assume that our input is analogous to the one of the last step of the topology-shape-metrics approach. We first present our reduction for the smooth orthogonal drawing model and afterwards we describe the required modifications for the corresponding reduction for the octilinear model.

Theorem 4 *Given a planar graph G of maximum vertex degree* 4 *and a smooth orthogonal representation $\mathcal{R}$, it is $\mathcal{NP}$-hard to decide whether G admits a bendless smooth orthogonal drawing preserving $\mathcal{R}$. This holds even if $\mathcal{R}$ requires all edges to be drawn as straight-line segments or quarter circular arcs.*

Proof Our reduction is from the well-known 3-SAT problem [25]. Given a 3-SAT formula φ in conjunctive normal form, we construct a graph G_φ and a smooth orthogonal representation $\mathcal{R}_\varphi$, such that G_φ admits a bendless smooth orthogonal drawing Γ_φ preserving $\mathcal{R}_\varphi$ if and only if formula φ is satisfiable; see also Fig. 12.

The main ideas of our construction are: (i) specific straight-line edges in Γ_φ transport *information* encoded in their length, (ii) rectangular faces of Γ_φ propagate the edge length of one side to its opposite side, and (iii) for a face composed of two straight-line edges and a quarter circular arc, the straight-line edges are of same length, which allows us to change the *direction* in which the information "flows".

Variable Gadget For each variable x of φ, we introduce a gadget, which is illustrated in Fig. 13. The bold-drawn quarter circular arc ensures that the sum of the edge lengths to its left is the same as the sum of the edge lengths to its bottom (refer to the edges with gray endvertices). As "input" the gadget gets three edges of unit length $\ell(u)$. This ensures that $\ell(x) + \ell(\overline{x}) = 3 \cdot \ell(u)$ holds for the "output literals" x and $\overline{x}$, where $\ell(x)$ and $\ell(\overline{x})$ denote the lengths of two edges representing x and $\overline{x}$.

To introduce our concept, assume that the lengths of all straight-line edges are integral and at least 1. If we could require $\ell(u) = 1$, then $\ell(x), \ell(\overline{x}) \in \{1, 2\}$. This would allow us to encode the assignment $x = \texttt{true}$ with $\ell(x) = 2$ and $\ell(\overline{x}) = 1$, and the assignment $x = \texttt{false}$ with $\ell(x) = 1$ and $\ell(\overline{x}) = 2$ (i.e., a length of 2 implies that the literal is true). However, if we cannot avoid, e.g., that $\ell(u) = 2$, then the variable gadget would not prevent us from setting $\ell(x) = \ell(\overline{x}) = 3$, which means that x and $\overline{x}$ are "half-true". We solve this issue by introducing the so-called *parity gadget*, that allows us to relax the integer constraint and to ensure that $\ell(x), \ell(\overline{x}) \in \{\ell(u) + \varepsilon,\ 2\ell(u) - \varepsilon\}$, for $\varepsilon << \ell(u)$.

Parity Gadget For each variable x of φ, graph G_φ has a gadget, which results in overlaps in Γ_φ, if the values of $\ell(x)$ and $\ell(\overline{x})$ do not differ significantly. For an illustration, refer to Fig. 14. The central part of this gadget is a "*vertical gap*" of width $3 \cdot \ell(u)$ (shaded in gray in Fig. 14a–c) with two blocks of vertices (triangular- and square-shaped in Fig. 14b–c) pointing inside the gap; a more detailed illustration of the vertical gap is given in Fig. 14c. Each block defines two square-shaped faces and

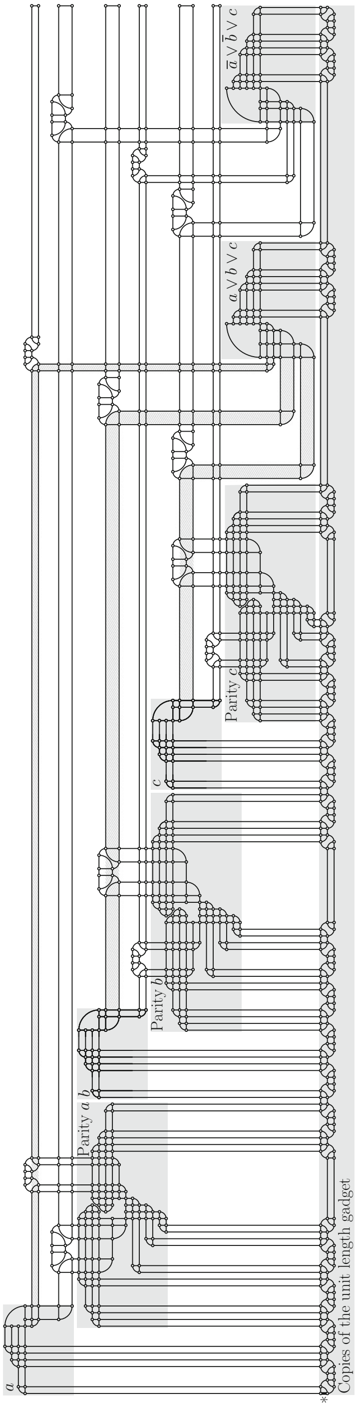

Fig. 12 Drawing Γ_φ for $\varphi = (a \vee b \vee c) \wedge (\overline{a} \vee \overline{b} \vee c)$ and the assignment $a =$ `false` and $b = c =$ `true`

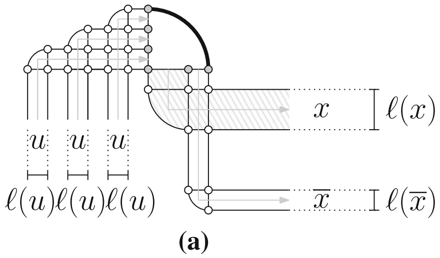

Fig. 13 The variable gadget; gray-colored arrows show the information "flow". **a** True state: $\ell(x) = 2$, $\ell(\overline{x}) = 1$. **b** False state: $\ell(x) = 1$, $\ell(\overline{x}) = 2$

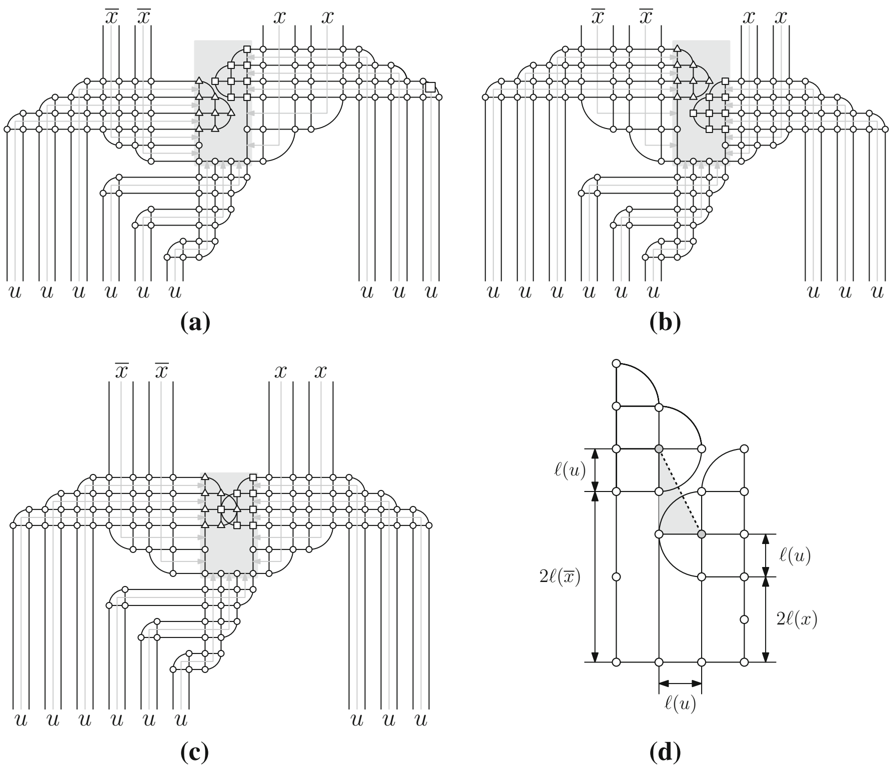

Fig. 14 The parity gadget; gray-colored arrows show the information "flow". **a** $x = \texttt{true}$. **b** $x = \texttt{false}$. **c** $\ell(x) \approx \ell(\overline{x})$. **d** Detail

three triangular faces, each formed by two straight-line edges and a quarter circular arc. Depending on the choice of $\ell(x)$ and $\ell(\overline{x})$, one of the blocks may be located above the other. If $\ell(x) \approx \ell(\overline{x})$, however, the two blocks are not far enough apart from each other leading to overlaps; see Fig. 14c.

Consider the case where $x = \texttt{false}$. The case where $x = \texttt{true}$ is symmetric. If $x = \texttt{false}$, we have to ensure that the two quarter circular arcs that are intersected by the dashed diagonal line-segment of Fig. 14d do not introduce crossings, i.e., in other

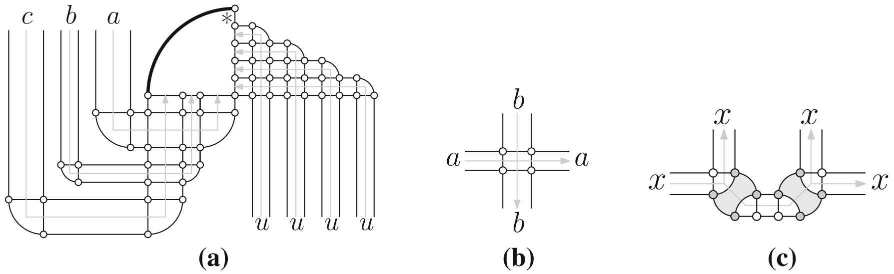

Fig. 15 Different gadgets; gray-colored arrows show the information "flow". **a** Clause gadget. **b** Crossing gadget. **c** Copy gadget

words the top one should be located on top of the bottom one in Fig. 14d. Since we know that both of these arcs have radius $\ell(u)$, their centers (gray-colored in Fig. 14d) should be at a distance greater than $2 \cdot \ell(u)$ apart from each other, i.e., the length of the dashed diagonal line segment is at least $2 \cdot \ell(u)$. However, the length of this segment can be easily expressed in dependence of $\lambda = \ell(\overline{x}) - \ell(x)$ as follows: $\sqrt{4\lambda^2 + \ell(u)^2}$. Hence, in order to avoid crossings it is not difficult to see that $\lambda > \sqrt{3}/2 \cdot \ell(u) \approx 0.866 \cdot \ell(u)$. This implies that $\ell(x), \ell(\overline{x}) \in (0,\ 1.067 \cdot \ell(u)) \cup (1.933 \cdot \ell(u),\ 3)$, i.e., $\varepsilon < 0.067 \cdot \ell(u)$ to avoid crossings.

Clause Gadget For each clause of φ with literals a, b and c, we introduce a gadget, which is illustrated in Fig. 15a. The bold-drawn quarter circular arc of Fig. 15a compares two sums of information. From the righthand side, four edges of unit length "enter" the arc. Observe that there is also a *free edge* (marked with an asterisk in Fig. 15a), which also contributes to the sum. Hence, the sum of edge lengths on the righthand side of this arc is greater than $4 \cdot \ell(u)$, since the free edge must have non-zero length. The three literals "enter" at the bottom; the sum here is $\ell(a) + \ell(b) + \ell(c)$. Combining both, we obtain that $\ell(a) + \ell(b) + \ell(c) > 4 \cdot \ell(u)$ must hold. The bold-drawn quarter circular arc of Fig. 15a implies that the length of the free edge must be equal to the difference between the two sides of this inequality. Also, note that not all a, b and c can be `false`, since in this case $\ell(a) + \ell(b) + \ell(c) = 3 \cdot (\ell(u) + \varepsilon) < 4 \cdot \ell(u)$, because $\varepsilon << \ell(u)$. However, if at least one literal is `true`, then $\ell(a) + \ell(b) + \ell(c) \geq 4 \cdot \ell(u) + \varepsilon$ and our inequality holds.

Auxiliary Gadgets The *crossing gadget* just consists of a rectangle and is used to allow two flows of information to cross each other; see Fig. 15b. The *copy gadget* takes an information and creates three copies of this information; see Fig. 15c. This is because the vertices of each gray colored quadrilateral face in Fig. 15c must be located at the corners of a rectangle whose sides have slopes ± 1, which implies that its opposite sides must be of the same length. Finally, the *unit length gadget* is a single edge, which we assume to have length $\ell(u)$. In Fig. 12, the unit length gadget is marked with an asterisk.

Description of the Construction We now describe our construction; see Fig. 12. Graph G_φ contains one unit length gadget, which is copied $O(\nu + \mu)$ times using the copy gadget, where ν and μ denote the number of variables and clauses of φ, respectively (since each variable and each clause introduces six and two copies of the copy gadget, respectively). For each variable of φ, graph G_φ has a variable gadget and a parity gadget, each of which is connected to different copies of the unit length gadget. For each clause of φ, graph G_φ has a clause gadget, which has four connections to different copies of the unit length gadget. We compute $\mathcal{R}_\varphi$ as follows. We place the variable gadget of each variable x above and to the left of its parity gadget and we connect the output literals of the variable gadget of x with its parity gadget through a copy gadget. We place the variable and the parity gadgets of the i-th variable below and to the right of the corresponding ones of the $(i-1)$-th variable. We place each clause gadget to the right of the sketch constructed so far, so that the gadget of the i-th clause is to the right of the $(i-1)$-th clause. This allows us to connect copies of the output literals of the variable gadget of each variable with the clause gadgets that contain it, so that all possible crossings (which are resolved using the crossing gadget) appear above the clause gadgets. More precisely, if a clause contains a literal of the i-th variable, we have a crossing with the literals of all variables with indices $(i+1)$ to ν. Hence, for each clause we add $O(\nu)$ crossing and three copy gadgets. Note that all copy gadgets of the unit length gadget lie below all variable, parity, and clause gadgets. The obtained representation $\mathcal{R}_\varphi$ conforms with the one of Fig. 12. Since the order of the variable and clause gadgets can be arbitrarily chosen in advance, we can assume that their connections are fixed, which implies that we know in advance the number and the positions of the required copy and crossing gadgets. Since, as already mentioned, for each clause we add $O(\nu)$ crossing gadgets, the construction can be done in $O(\nu\mu)$ time.

To complete the proof, assume that graph G_φ admits a bendless smooth orthogonal drawing Γ_φ preserving $\mathcal{R}_\varphi$. We compute a truth assignment for φ as follows. For each variable x of φ, we set x to `true` if and only if $\ell(x) \geq 1.933 \cdot \ell(u)$. Since for each clause $(a \vee b \vee c)$ of φ we have that $\ell(a) + \ell(b) + \ell(c) > 4 \cdot \ell(u)$, it follows that at least one of a, b and c must be `true`. Hence, φ admits a truth assignment. For the opposite direction, based on a truth assignment of φ, we can set, e.g., $\ell(x) = 1.95$ and $\ell(\overline{x}) = 1.05$ for each variable x, assuming that $\ell(u) = 1$. Then, arranging the variable and the clause gadgets of G_φ as in Fig. 12 yields a bendless smooth orthogonal drawing Γ_φ preserving $\mathcal{R}_\varphi$. □

Remark 1 The special case of our problem, in which circular arcs are not present, is closely related to the so-called *HV-rectilinear planarity testing* [34]. In this problem, each edge has either an H- or a V-label and the goal is to determine whether there exist a rectilinear drawing in which all edges with an H-label are drawn as horizontal segments, while all edges with an V-label are drawn as vertical segments. As opposed to our problem, HV-rectilinear planarity testing is polynomial-time solvable in the fixed embedding setting [20] (note that the angles around each vertex are not specified as part of the input of the problem) and becomes $\mathcal{NP}$-hard in the variable embedding setting [16].

We now proceed to prove the analogous of Theorem 4 for the octilinear model.

Theorem 5 *Given a planar graph G of maximum vertex degree 4 and an octilinear representation $\mathcal{R}$, it is $\mathcal{NP}$-hard to decide whether G admits a bendless octilinear drawing preserving $\mathcal{R}$.*

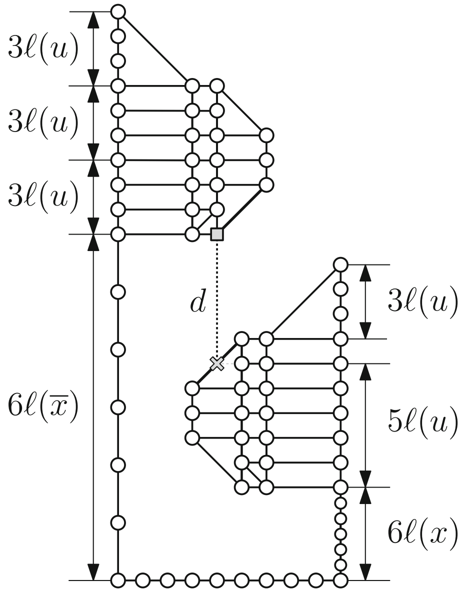

Fig. 16 The parity gadget for the octilinear model

Proof In principle, our proof follows the same reduction scheme as the one of Theorem 4. More precisely, we can adjust to the octilinear model by replacing quarter circular arcs with diagonal segments. By doing so, we maintain planarity (by construction). However, the parity gadget has to be adjusted properly, so to maintain its functionality. To this end, we only change the vertical gap of parity gadget as in Fig. 16, which shows the case where $x = \texttt{false}$; the case where $x = \texttt{true}$ is symmetric.

It is not difficult to see that the smallest vertical distance d between the blocks in the vertical gap (illustrated as a dotted line-segment in Fig. 16) equals to $6\ell(\overline{x}) - 6\ell(x) - 5\ell(u)$, which implies $\ell(\overline{x}) - \ell(x) > 5/6 \cdot \ell(u)$, since d must be strictly greater than zero. Thus, $\varepsilon < 0.084 \cdot \ell(u) << \ell(u)$. □

5 Bi-Monotone Drawings

In this section, we study variants of the *Kandinsky* drawing model [7,14,23], which forms an extension of the orthogonal model to graphs of vertex degree greater than 4. In this model, the vertices are represented as squares, placed on a *coarse grid* with multiple edges attached to each side of them aligned on a *finer grid*. Since Kandinsky drawings find applications in diverse areas, such as VLSI design, UML diagrams and business process modeling, this drawing model has been extensively studied over the years; see, e.g., [9,10].

The Kandinsky model allows for natural extensions to both smooth orthogonal and octilinear models. We are aware of only one preliminary result in this direction for the former model: A linear time drawing algorithm is presented in [5] for the production of smooth orthogonal 2-drawings for planar graphs of arbitrary vertex degree in quadratic

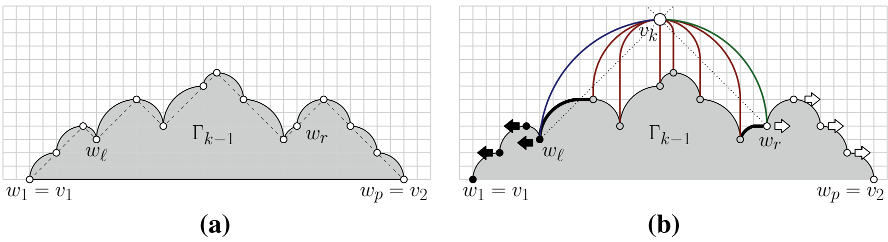

Fig. 17 Illustration of the modified shift-method for the smooth orthogonal model. **a** Contour condition. **b** Placement of v_k in Γ_{k-1}

area, in which all vertices are on a line ℓ and the edges are drawn either as half circles (above or below ℓ), or as two consecutive half circles one above and one below ℓ (that is, the latter ones are of complexity 2, but they are at most $\lfloor(n-3)/2\rfloor$ [11]).

For an input maximal planar graph G (of arbitrary vertex degree), our goal is to construct a smooth orthogonal (or an octilinear) 2-drawing for G with the following aesthetic benefits over the aforementioned drawing algorithm:

(i) the vertices are not restricted along a line, and
(ii) each edge is *bi-monotone* [24], i.e., xy-monotone.

We achieve our goal at the cost of slightly more edges drawn with complexity 2 or at the cost of increased drawing area (but still polynomial).

Our first approach is a modification of the *shift-method* [13] (see also Sect. 2). Based on a canonical order $\pi = (v_1, \ldots, v_n)$ of G, we construct a planar smooth orthogonal 2-drawing Γ of G in the Kandinsky model, as follows. We place v_1, v_2 and v_3 at points $(0, 0)$, $(2, 0)$ and $(1, 1)$, respectively. Hence, we can draw edge (v_1, v_2) as a horizontal line-segment, and each of edges (v_1, v_3) and (v_2, v_3) as a quarter circular arc. We also color edge (v_1, v_3) blue and edge (v_2, v_3) green; edges of the same color will eventually be drawn in the same manner. For $k = 4, \ldots, n$, assume that a smooth orthogonal 2-drawing Γ_{k-1} of the subgraph G_{k-1} of G induced by $v_1, \ldots, v_{k-1}$ has been constructed, in which each edge of the outerface C_{k-1} of Γ_{k-1} is drawn as a quarter circular arc, whose endvertices are on a line with slope ± 1, except for edge (v_1, v_2), which is drawn as a horizontal segment (called *contour condition* in the shift-method). For an illustration, refer to Fig. 17a. Each of $v_1, \ldots, v_{k-1}$ is also associated with a so-called *shift-set*, which for v_1, v_2 and v_3 are singletons containing only themselves (as in the shift-method).

Let $(w_1, \ldots, w_p)$ be the vertices of C_{k-1} from left to right in Γ_{k-1}, where $w_1 = v_1$ and $w_p = v_2$. Let $(w_\ell, \ldots, w_r)$, $1 \le \ell < r \le p$, be the neighbors of v_k from left to right along C_{k-1} in Γ_{k-1}. As in the shift-method, our algorithm first translates each vertex in $\cup_{i=1}^{\ell} S(w_i)$ one unit to the left and each vertex in $\cup_{i=r}^{p} S(w_i)$ one unit to the right, where $S(v)$ is the shift-set of $v \in V$. During this translation, each of edges $(w_\ell, w_{\ell+1})$ and (w_{r-1}, w_r) acquires a horizontal segment (see the bold edges of Fig. 17b). We place vertex v_k at the intersection of line λ_ℓ with slope $+1$ through w_ℓ with line λ_r with slope -1 through w_r (which are drawn dotted in Fig. 17b) and we set the shift-set of v_k to $\{v_k\} \cup_{i=\ell+1}^{r-1} S(w_i)$, as in the shift-method. We draw each of edges (w_ℓ, v_k) and (v_k, w_r) as a quarter circular arc. The remaining edges incident to v_k are drawn with complexity 2. More precisely, for $i = \ell + 1, \ldots, r - 1$, edge

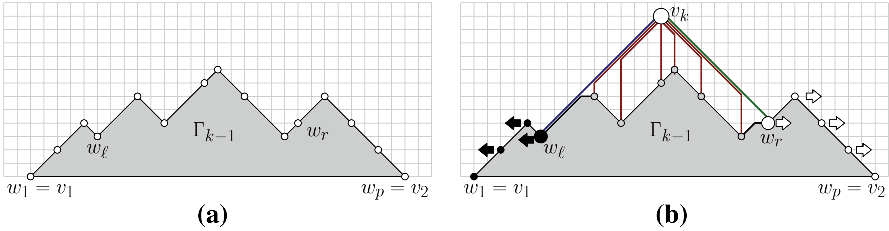

Fig. 18 Illustration of the modified shift-method for the octilinear model. **a** Contour condition. **b** Placement of v_k in Γ_{k-1}

(w_i, v_k) has a vertical line-segment that starts from w_i and ends either at λ_ℓ or λ_r and a quarter circular arc from the end of the previous segment to v_k. Hence, the contour condition is satisfied.

We color edge (w_ℓ, v_k) blue, edge (v_k, w_r) green and the remaining edges incident to v_k in G_k red (this type of coloring is also known as *Schnyder coloring* [22,37]). Observe that each blue and green edge consists of a quarter circular arc and a horizontal segment (that may have zero length), while a red edge consists of a vertical segment and a quarter circular arc (that may have zero radius). We are now ready to state the following theorem.

Theorem 6 *A maximal planar n-vertex graph admits a bi-monotone planar smooth orthogonal* 2*-drawing in the Kandinsky model, which requires* $O(n^2)$ *area and can be computed in* $O(n)$ *time.*

Proof Bi-monotonicity and the fact that the computed drawing is a 2-drawing follows by construction. The time complexity follows from [12]. Planarity is proven by induction. Drawing Γ_3 is planar by construction. Assuming that Γ_{k-1} is planar, we observe that no two edges incident to v_k cross in Γ_k. Also, these edges do not cross edges of Γ_{k-1}. Since the radii of the arcs of the edges incident to vertices that are shifted remain unchanged and since edges incident to vertices in the shift-sets retain their shape, drawing Γ_k is planar. This completes our proof. □

For the octilinear model, we can analogously state the following theorem.

Theorem 7 *A maximal planar n-vertex graph admits a bi-monotone planar octilinear* 2*-drawing in the Kandinsky model, which requires* $O(n^2)$ *area and can be computed in* $O(n)$ *time. Additionally, each bend is at* 135°.

Proof We can convert the layout computed for the smooth orthogonal model to octilinear by redrawing all its quarter circular arcs to diagonal segments; see also Fig. 18b. This results in bends at 135°. Planarity follows from the fact that blue and green edges do not pass through vertices by construction. □

We reduce the number of edges drawn with complexity 2, by computing new y-coordinates for the vertices, while keeping their x-coordinates unchanged. To achieve this, we process the vertices of G in the same canonical ordering $\pi = (v_1, \ldots, v_n)$ maintaining the following invariant (which is a modification of the contour condition):

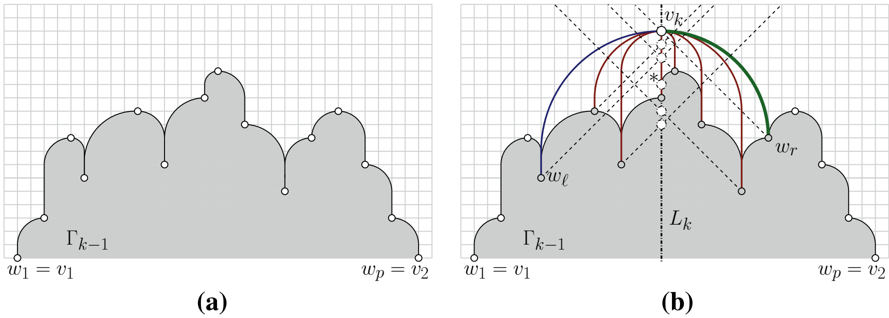

Fig. 19 Illustration of the contour condition and placement of v_k in Γ_{k-1}. **a** Invariant 1. **b** Placement of v_k in Γ_{k-1}

(I.1) Each edge of the outerface has a quarter circular arc segment of non-zero radius, except for the edge (v_1, v_2); see Fig. 19a.

Initially, we set $y(v_1) = y(v_2) = 0$. For $k = 3, \dots, n$, we assume as in the shift-method that the neighbors of vertex v_k in Γ_{k-1} are $(w_\ell, \dots, w_r)$ from left to right along C_{k-1}. Next, from each of the vertices $w_\ell, \dots, w_r$ that are strictly to the left (right) of v_k, we draw a line with slope $+1$ (-1, resp.); refer to the dashed drawn lines of Fig. 19b. The intersections of these lines with the vertical line $L_k : x = x(v_k)$ are *candidate positions* for the placement of v_k. If there is a vertex w_i, for some $i = \ell, \dots, r$, whose x-coordinate is equal to the x-coordinate of vertex v_k (that is, $x(w_i) = x(v_k)$), then there is one more candidate position, called *trivial*, for the placement of v_k, which is also along the line L_k at $(x(w_i), y(w_i) + 1)$; refer to the candidate position marked with an asterisk in Fig. 19b. We choose to place v_k at the highest candidate position. More precisely, let $\Delta_x(u, v)$ be the horizontal distance between vertices u and v. Then, formally, the y-coordinate of vertex v_k is computed as follows:

$$y(v_k) = \max_{w \in \{w_\ell, \dots, w_r\}} \{y(w) + \max\{\Delta_x(v_k, w), 1\}\} \tag{1}$$

Let $w^* \in \{w_\ell, \dots, w_r\}$ be the vertex of C_{k-1} defining the highest candidate position. Note that, in general, more than one vertex may define the highest candidate position. It is not difficult to see that edge (v_k, w^*) can be drawn as a quarter circular arc, unless v_k is placed in the trivial candidate position, in which case we draw it as a vertical line-segment of unit length. This immediately implies that (at least) $n - 1$ edges are drawn with complexity 1, as desired. We draw the remaining edges incident to v_k with complexity 2. More precisely, each of these edges is composed of two segments; one quarter circular arc segment incident to v_k followed by a vertical line-segment incident to the other endpoint. Since $x(w_\ell) < x(v_k) < x(w_r)$, it follows that Invariant 1 is maintained, by construction; in addition, note that the quarter circular arc of Invariant 1 is always incident to vertex v_k. We are now ready to state the following theorem.

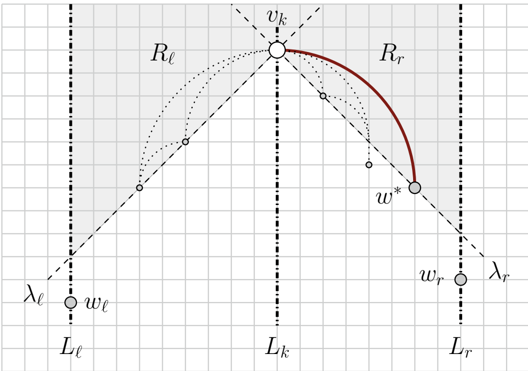

Fig. 20 Illustration for the proof of Theorem 8

Theorem 8 *A maximal planar n-vertex graph G admits a bi-monotone planar smooth orthogonal 2-drawing Γ with at least $n - 1$ edges drawn with complexity 1 in the Kandinsky model, which requires $O(n^3)$ area and can be computed in $O(n)$ time.*

Proof The time complexity follows from the shift-method. Since the fact that at least $n-1$ edges are drawn with complexity 1 has already been discussed, in order to prove this theorem, it remains to show that the computed drawing is planar and that its area is cubic. The latter can be proven immediately. Since the horizontal distance between any two vertices of G in Γ is $O(n)$, it follows that the vertical distance between any two consecutive (in the canonical ordering) vertices in Γ cannot be more than $O(n)$, which implies that the height of Γ is at most $O(n^2)$. Hence, the area occupied by Γ is $O(n^3)$.

We prove planarity inductively. For the base of the induction, note that drawing Γ_3 is planar. Assuming that Γ_{k-1} is planar, we show in the following that Γ_k is planar, as well. By construction, the edges that are incident to v_k do not cross each other. This is because of Invariant 1, which ensures that no two neighbors of v_k in G_k have the same x-coordinate. Since drawing Γ_{k-1} remains unchanged after placing v_k (and hence planar as subdrawing of Γ_k), it remains to prove that the edges incident to v_k do not introduce crossings with edges of Γ_{k-1}; in particular with edges of C_{k-1}.

Let L_ℓ and L_r be the vertical lines through w_ℓ and w_r in Γ_k, respectively; see Fig. 20. By construction, there is no vertex in the region R_ℓ between L_ℓ and L_k that lies above the line λ_ℓ with slope $+1$ through v_k. Symmetrically, there is no vertex in the region R_r between L_k and L_r that lies above the line λ_r with slope -1 through v_k; both regions R_ℓ and R_r are highlighted in gray in Fig. 20. However, along the parts of λ_ℓ and λ_r that lie in the interior of R_ℓ and R_r, respectively, there might exist several vertices (one of them is w^*).

Since w_ℓ and w_r are the leftmost and rightmost neighbors of v_k in Γ_{k-1}, it follows that the neighbors $w_\ell, \dots, w_r$ of v_k in G_k lie between L_ℓ and L_r (and either completely below or along λ_ℓ and λ_r). Each edge incident to v_k in G_k has a circular arc segment that starts from v_k and ends at a point along λ_ℓ or λ_r (followed by a vertical segment of possibly zero length towards one of $w_\ell, \dots, w_r$), such that no two such circular arc segments overlap, as by Invariant 1 no two vertices among $w_\ell, \dots, w_r$ have the same

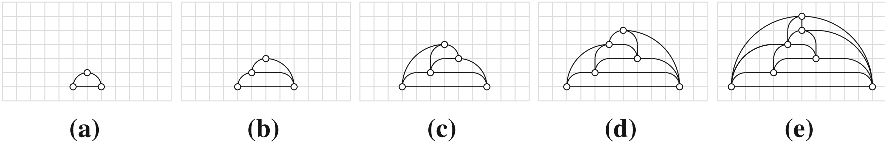

Fig. 21 The steps of drawing a planar graph with our modified shift-method

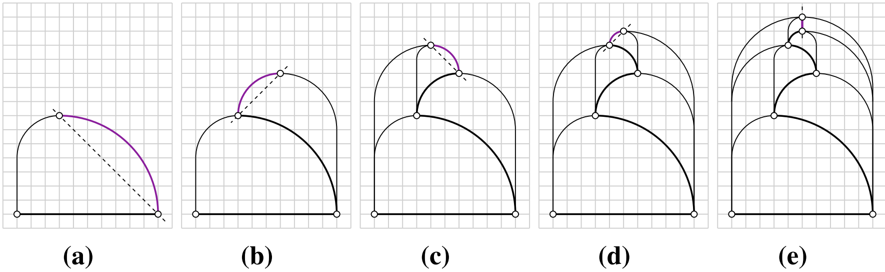

Fig. 22 Illustration of the reduction of the number of edges drawn with complexity 2

x-coordinate. Since in regions R_ℓ and R_r there are no vertices of G_k, it follows that these circular arcs may only cross other circular arc segments that lie in R_ℓ and R_r, which must have both endpoints either along λ_ℓ or along λ_r. However, such crossings are not possible because the radius of the circular arc segment of an edge (w_i, w_{i+1}) of C_{k-1} is smaller than the radius of the circular arc segments of both edges (v_k, w_i) and (v_k, w_{i+1}) in such a scenario; refer to the dotted drawn edges of Fig. 20. Since the vertical edge segments incident to each of $w_\ell, \ldots, w_r$ neither cross each other nor cross edges of C_{k-1}, it follows that Γ_k is in fact planar. □

6 Example Run of our Drawing Algorithm

In this section, we describe an example run of our drawing algorithm from Sect. 5 on a planar triangulation on seven vertices. Figure 21 shows the steps of constructing a smooth orthogonal drawing of this graph using our modification of the shift-method.

Figure 22 illustrates how new y-coordinates are assigned to the vertices so to reduce the number of edges drawn with complexity 2 (observe that the x-coordinates are the ones of Fig. 21e). In particular, Fig. 22a shows how this is done for the first three vertices. Figure 22b–e illustrate how the fourth, the fifth, the sixth and the seventh vertex of the graph is added. The bold edges in each subfigure of Fig. 22 are the ones defining the y-coordinate which are drawn with complexity 1 at each step of the canonical order. The final drawing is the one of Fig. 22e. We emphasize on the additional area consumption, which on the vertical dimension increases to quadratic.

7 Conclusions

In this paper, we continued the study of smooth orthogonal and octilinear drawings. Our $\mathcal{NP}$-hardness proofs are a first step towards settling the complexity of both drawing problems. It is interesting to study whether any of the two problems also belongs to $\mathcal{NP}$. We further conjecture that deciding whether a planar graph admits a bendless smooth orthogonal drawing is $\mathcal{NP}$-hard, even in the case where only the planar embedding is specified by the input. For the octilinear drawing problem, it is of interest to know if it remains $\mathcal{NP}$-hard even for planar graphs of maximum vertex degree 4 or if these graphs allow for a decision algorithm. Our drawing algorithms guarantee bi-monotone 2-drawings with a certain number of complexity-1 edges for maximal planar graphs. Improvements or generalizations to non-triangulated planar graphs are of importance.

Acknowledgements This work has been supported by DFG Grant Ka812/17-1. The authors would like to thank Patrizio Angelini and Martin Gronemann for useful discussions. We would also like to thank the anonymous reviewers for useful comments.

References

1. Alam, M.J., Bekos, M.A., Kaufmann, M., Kindermann, P., Kobourov, S.G., Wolff, A.: Smooth orthogonal drawings of planar graphs. In: Pardo, A., Viola, A. (eds.) LATIN, Volume 8392 of LNCS, pp. 144–155. Springer, Berlin (2014)
2. Bekos, M.A., Förster, H., Kaufmann, M.: On smooth orthogonal and octilinear drawings: relations, complexity and kandinsky drawings. In: Frati, F., Ma, K.-L. (eds.) Graph Drawing, Volume 10692 of LNCS, pp. 169–183. Springer, Berlin (2017)
3. Bekos, M.A., Gronemann, M., Kaufmann, M., Krug, R.: Planar octilinear drawings with one bend per edge. J. Graph Algorithms Appl. **19**(2), 657–680 (2015)
4. Bekos, M.A., Gronemann, M., Pupyrev, S., Raftopoulou, C.N.: Perfect smooth orthogonal drawings. In: Bourbakis, N.G., Tsihrintzis, G.A., Virvou, M. (eds.) IISA, pp. 76–81. IEEE (2014)
5. Bekos, M.A., Kaufmann, M., Kobourov, S.G., Symvonis, A.: Smooth orthogonal layouts. J. Graph Algorithms Appl. **17**(5), 575–595 (2013)
6. Bekos, M.A., Kaufmann, M., Krug, R.: On the total number of bends for planar octilinear drawings. J. Graph Algorithms Appl. **21**(4), 709–730 (2017)
7. Bertolazzi, P., Di Battista, G., Didimo, W.: Computing orthogonal drawings with the minimum number of bends. IEEE Trans. Comput. **49**(8), 826–840 (2000)
8. Biedl, T.C., Kant, G.: A better heuristic for orthogonal graph drawings. Comput. Geom. **9**(3), 159–180 (1998)
9. Bläsius, T., Krug, M., Rutter, I., Wagner, D.: Orthogonal graph drawing with flexibility constraints. Algorithmica **68**(4), 859–885 (2014)
10. Bläsius, T., Lehmann, S., Rutter, I.: Orthogonal graph drawing with inflexible edges. Comput. Geom. **55**, 26–40 (2016)
11. Cardinal, J., Hoffmann, M., Kusters, V., Tóth, C.D., Wettstein, M.: Arc diagrams, flip distances, and hamiltonian triangulations. CoRR, arXiv:1611.02541 (2016)
12. Chrobak, M., Payne, T.H.: A linear-time algorithm for drawing a planar graph on a grid. Inf. Process. Lett. **54**(4), 241–246 (1995)
13. de Fraysseix, H., Pach, J., Pollack, R.: How to draw a planar graph on a grid. Combinatorica **10**(1), 41–51 (1990)
14. Di Battista, G., Didimo, W., Patrignani, M., Pizzonia, M.: Orthogonal and quasi-upward drawings with vertices of prescribed size. In: Kratochvíl, J. (ed.) Graph Drawing, Volume 1731 of LNCS, pp. 297–310. Springer, Berlin (1999)
15. Di Battista, G., Eades, P., Tamassia, R., Tollis, I.G.: Graph Drawing: Algorithms for the Visualization of Graphs. Prentice-Hall, Upper Saddle River (1999)
16. Didimo, W., Liotta, G., Patrignani, M.: On the complexity of HV-rectilinear planarity testing. In: Duncan, C.A., Symvonis, A. (eds.) Graph Drawing, Volume 8871 of LNCS, pp. 343–354. Springer, Berlin (2014)

17. Di Giacomo, E., Liotta, G., Montecchiani, F.: The planar slope number of subcubic graphs. In: Pardo, A., Viola, A. (eds.) LATIN, Volume 8392 of LNCS, pp. 132–143. Springer, Berlin (2014)
18. Duncan, C.A., Eppstein, D., Goodrich, M.T., Kobourov, S.G., Nöllenburg, M.: Lombardi drawings of graphs. J. Graph Algorithms Appl. **16**(1), 85–108 (2012)
19. Duncan, C.A., Goodrich, M.T.: Planar orthogonal and polyline drawing algorithms. In: Tamassia, R. (ed.) Handbook on Graph Drawing and Visualization, pp. 223–246. Chapman and Hall/CRC, Boca Raton (2013)
20. Durocher, S., Felsner, S., Mehrabi, S., Mondal, D.: Drawing HV-restricted planar graphs. In: Alberto, P., Alfredo, V. (eds.) LATIN, Volume 8392 of LNCS, pp. 156–167. Springer, Berlin (2014)
21. Eppstein, D.: Planar lombardi drawings for subcubic graphs. In: Didimo, W., Patrignani, M. (eds.) Graph Drawing, Volume 7704 of LNCS, pp. 126–137. Springer, Berlin (2012)
22. Felsner, S.: Geometric Graphs and Arrangements. Advanced Lectures in Mathematics. Vieweg, Berlin (2004)
23. Fößmeier, U., Kaufmann, M.: Drawing high degree graphs with low bend numbers. In: Brandenburg, F.-J. (ed.) Graph Drawing, Volume 1027 of LNCS, pp. 254–266. Springer, Berlin (1995)
24. Fulek, R., Pelsmajer, M.J., Schaefer, M., Stefankovic, D.: Hanani-tutte and monotone drawings. In: Kolman, P., Kratochvíl, J. (eds.) WG, Volume 6986 of LNCS, pp. 283–294. Springer, Berlin (2011)
25. Garey, M.R., Johnson, D.S.: Computers and Intractability: A Guide to the Theory of NP-Completeness. W. H. Freeman, New York (1979)
26. Garg, A., Tamassia, R.: On the computational complexity of upward and rectilinear planarity testing. SIAM J. Comput. **31**(2), 601–625 (2001)
27. Harary, F.: Graph Theory. Addison-Wesley, Boston (1991)
28. Hong, S.-H., Merrick, D., do Nascimento, H.A.D.: Automatic visualisation of metro maps. J. Vis. Lang. Comput. **17**(3), 203–224 (2006)
29. Kant, G.: Hexagonal grid drawings. In: Mayr, E.W. (ed.) WG, Volume 657 of LNCS, pp. 263–276. Springer, Berlin (1992)
30. Kant, G.: Drawing planar graphs using the canonical ordering. Algorithmica **16**(1), 4–32 (1996)
31. Kaufmann, M., Wagner, D. (eds.): Drawing Graphs, Methods and Models, Volume 2025 of LNCS. Springer, Berlin (2001)
32. Keszegh, B., Pach, J., Pálvölgyi, D.: Drawing planar graphs of bounded degree with few slopes. SIAM J. Discrete Math. **27**(2), 1171–1183 (2013)
33. Liu, Y., Morgana, A., Simeone, B.: A linear algorithm for 2-bend embeddings of planar graphs in the two-dimensional grid. Discrete Appl. Math. **81**(1–3), 69–91 (1998)
34. Manuch, J., Murray, P., Sheung-Hung, P., Thachuk, C.: Complexity of finding non-planar rectilinear drawings of graphs. In: Brandes, U., Cornelsen, S. (eds.) Graph Drawing, Volume 6502 of LNCS, pp. 305–316. Springer, Berlin (2010)
35. Nöllenburg, M.: Automated drawing of metro maps. Master's Thesis. Fakultät für Informatik, Universität Karlsruhe (TH) (August 2005)
36. Nöllenburg, M., Wolff, A.: Drawing and labeling high-quality metro maps by mixed-integer programming. IEEE Trans. Vis. Comput. Graph. **17**(5), 626–641 (2011)
37. Schnyder, W.: Embedding planar graphs on the grid. In: Johnson, D.S. (ed.) SODA, pp. 138–148. SIAM, San Francisco (1990)
38. Stott, J.M., Rodgers, P., Martinez-Ovando, J.C., Walker, S.G.: Automatic metro map layout using multicriteria optimization. IEEE Trans. Vis. Comput. Graph. **17**(1), 101–114 (2011)
39. Tamassia, R.: On embedding a graph in the grid with the minimum number of bends. SIAM J. Comput. **16**(3), 421–444 (1987)
40. Tamassia, R. (ed.): Handbook on Graph Drawing and Visualization. Chapman and Hall/CRC, Boca Raton (2013)